nature biotechnology

SUPPLEMENTARY INFORMATION

https://doi.org/10.1038/s41587-019-0104-4

In the format provided by the authors and unedited.

NRT1.1B is associated with root microbiota composition and nitrogen use in field-grown rice

Jingying Zhang[1,2,10], Yong-Xin Liu[1,2,10], Na Zhang[1,2,3,10], Bin Hu[1,10], Tao Jin[4,5,6,10], Haoran Xu[1,2,3], Yuan Qin[1,2,3], Pengxu Yan[4,5,6], Xiaoning Zhang[1,2,3], Xiaoxuan Guo[1,2], Jing Hui[7], Shouyun Cao[1], Xin Wang[1,2], Chao Wang[1,2], Hui Wang[1,2,3], Baoyuan Qu[1,2], Guangyi Fan[4,5,6], Lixing Yuan[7], Ruben Garrido-Oter[8,9], Chengcai Chu[1,3]* and Yang Bai[1,2,3]*

[1]State Key Laboratory of Plant Genomics, Institute of Genetics and Developmental Biology, The Innovative Academy of Seed Design, Chinese Academy of Sciences, Beijing, China. [2]CAS-JIC Centre of Excellence for Plant and Microbial Science, Institute of Genetics and Developmental Biology, Chinese Academy of Sciences, Beijing, China. [3]College of Advanced Agricultural Sciences, University of Chinese Academy of Sciences, Beijing, China. [4]BGI-Shenzhen, Shenzhen, China. [5]BGI-Qingdao, BGI-Shenzhen, Qingdao, China. [6]China National Genebank-Shenzhen, BGI-Shenzhen, Shenzhen, China. [7]Key Lab of Plant–Soil Interactions, MOE, College of Resources and Environmental Sciences, China Agricultural University, Beijing, China. [8]Department of Plant Microbe Interactions, Max Planck Institute for Plant Breeding Research, Cologne, Germany. [9]Cluster of Excellence on Plant Sciences, Dusseldorf, Germany. [10]These authors contributed equally: Jingying Zhang, Yong-Xin Liu, Na Zhang, Bin Hu, Tao Jin. *e-mail: ccchu@genetics.ac.cn; ybai@genetics.ac.cn

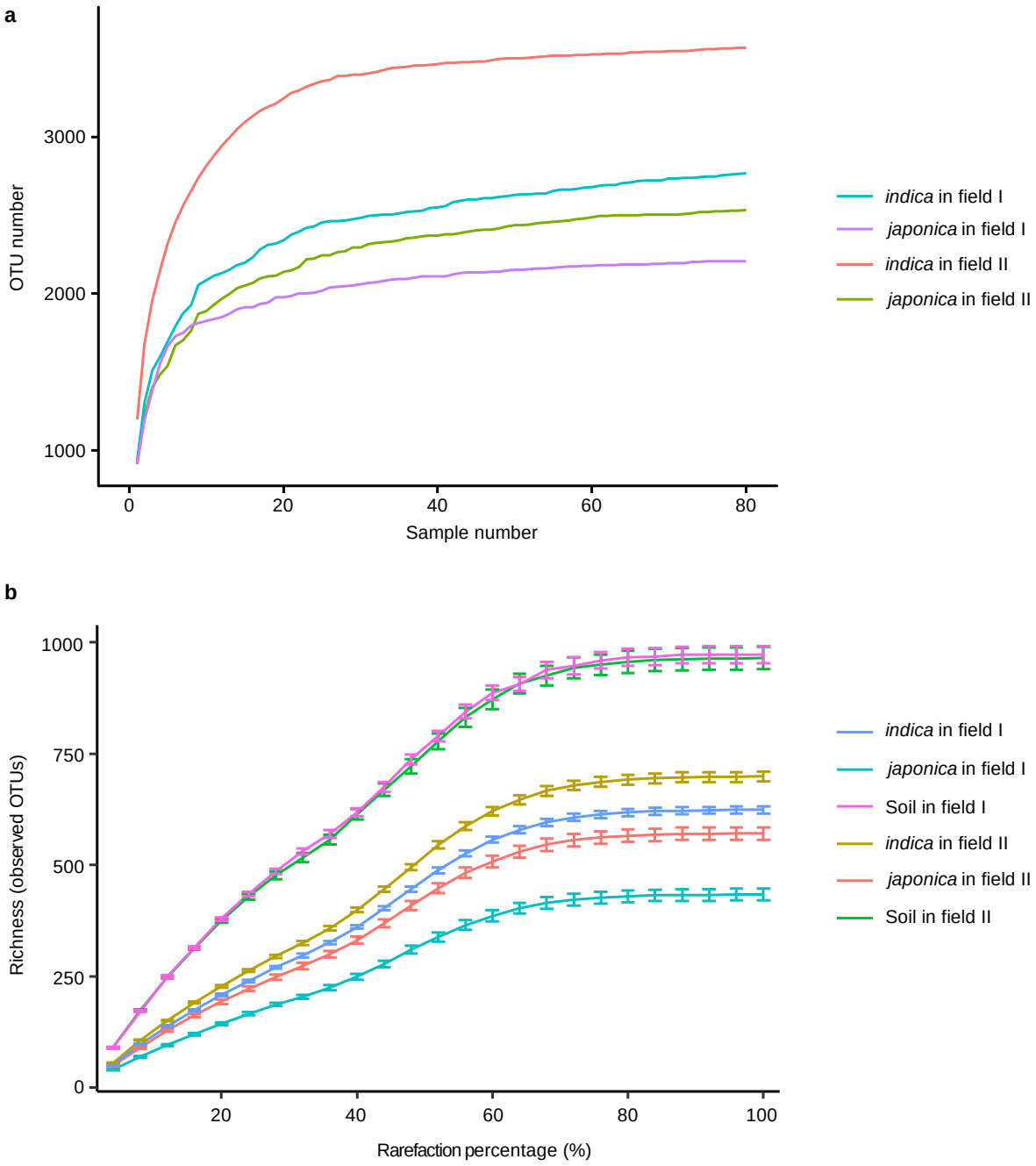

Supplementary Figure 1

Coverage of members in the root bacterial microbiota by the representative *indica* and *japonica* varieties.

(**a**) Rarefaction curves of detected bacterial species of the root microbiota reach the saturation stage with increasing numbers of samples, indicating that the root microbiota in our population capture most root bacteria members from each rice subspecies. *Indica* and *japonica* varieties in two locations are shown separately. (**b**) Rarefaction curves of detected bacterial OTUs of the root microbiota from *indica* and *japonica* varieties reach saturation stage with increasing sequencing depth. Each vertical bar represents standard error. The numbers of replicated samples in this figure are as follows: in field I, *indica* (*n* = 201), *japonica* (*n* = 80), soil (*n* = 12); in field II, *indica* (*n* = 201), *japonica* (*n* = 81), soil (*n* = 12).

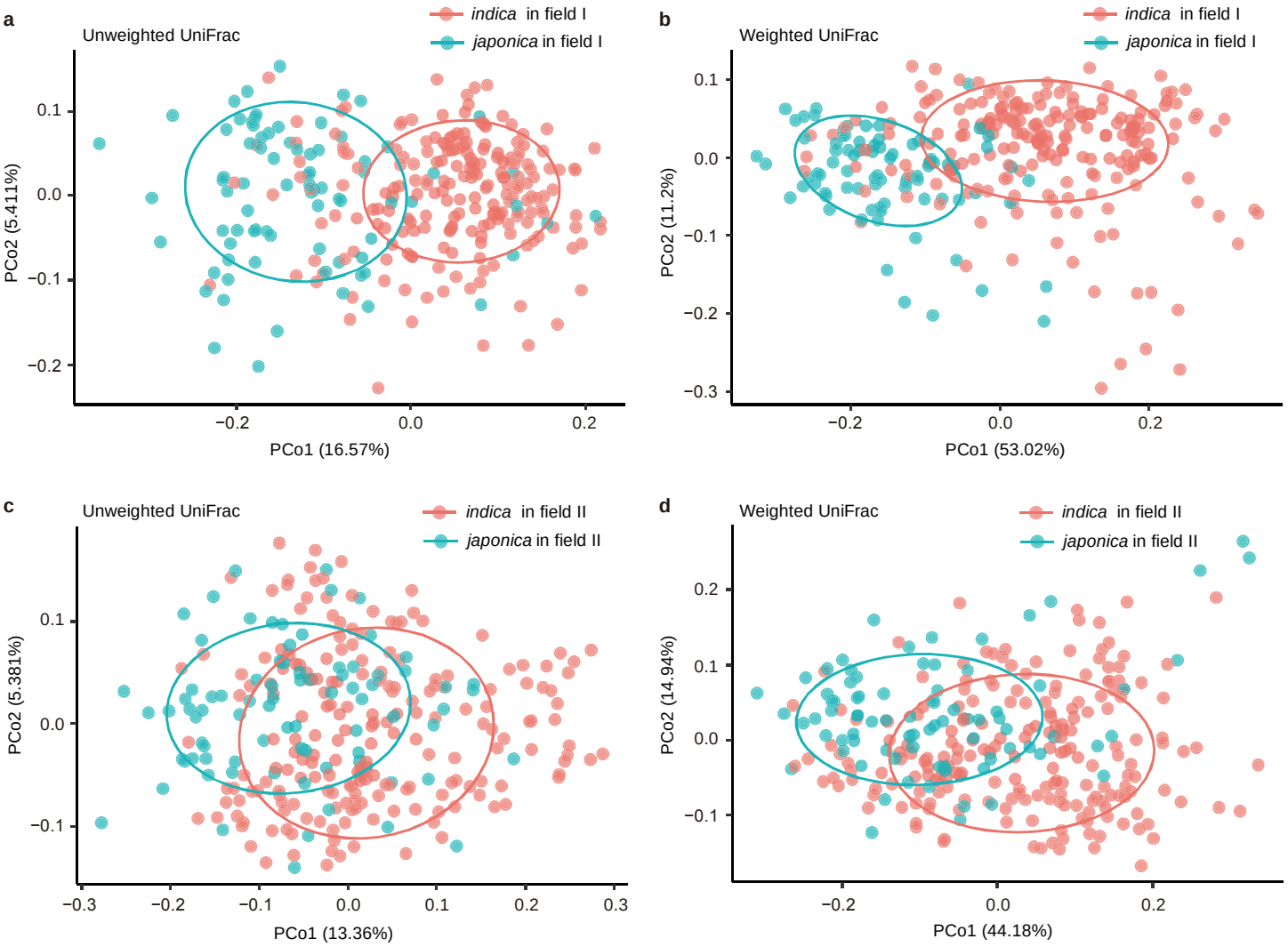

Supplementary Figure 2

Comparison of the root microbiota of *indica* and *japonica* varieties.

(**a**,**b**) Principal coordinate analysis with unweighted (**a**) and weighted (**b**) UniFrac distance show that the root microbiota of *indica* separate from that of *japonica* in field I in the first two axes, indicating that the root microbiota of *indica* are distinct from that of *japonica* ($P < 0.001$, PERMANOVA by Adonis). Ellipses cover 68% of the data for each rice subspecies. (**c**,**d**) Principal coordinate analysis with unweighted (**c**) and weighted (**d**) UniFrac distance showing that the root microbiota of *indica* separate from those of *japonica* in field II in the first two axes, revealing that root microbiota of *indica* are distinct from those of *japonica* ($P < 0.001$, PERMANOVA by Adonis). The numbers of replicated samples are as follows: in field I, *indica* ($n = 201$), *japonica* ($n = 80$); in field II, *indica* ($n = 201$), *japonica* ($n = 81$).

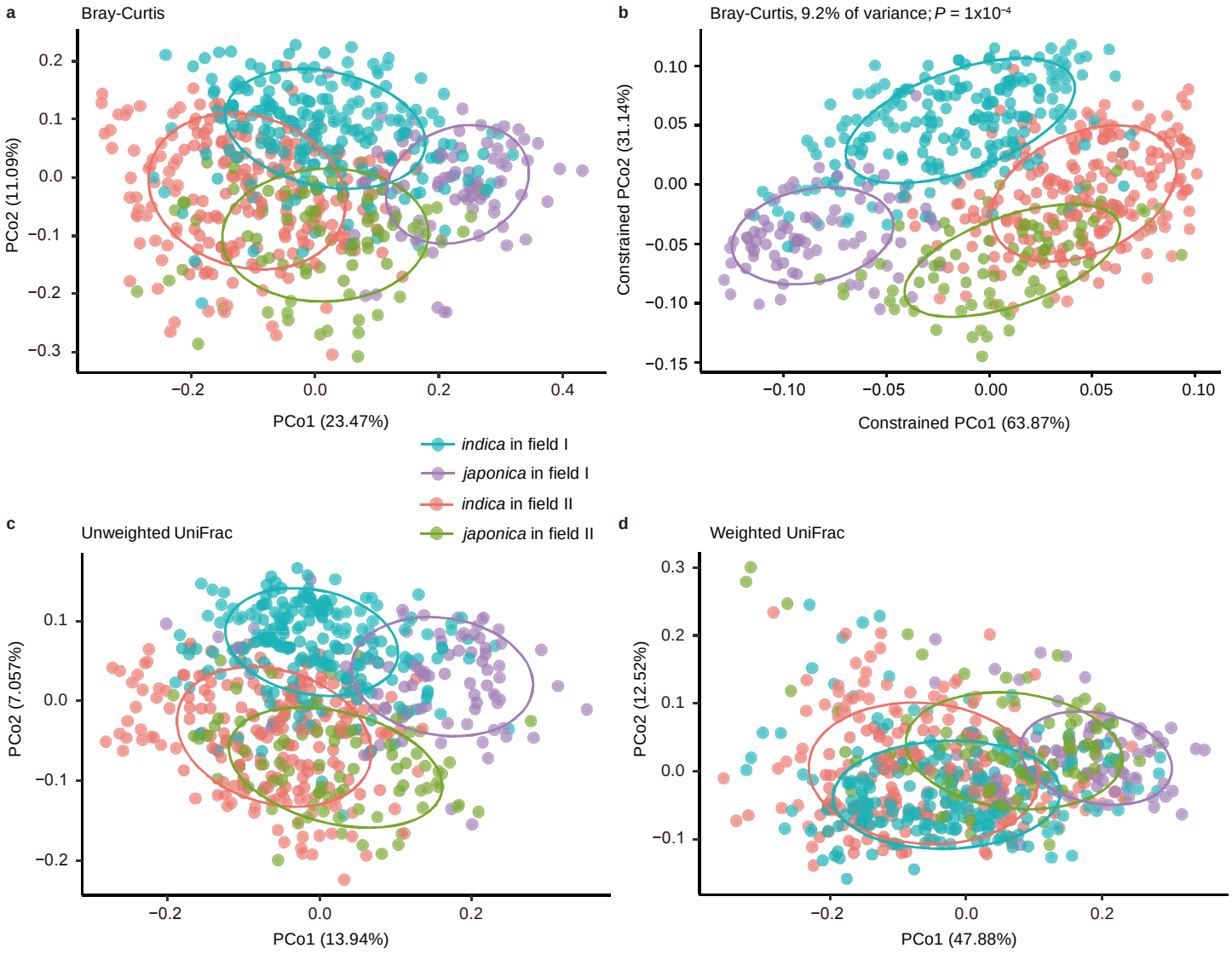

Supplementary Figure 3

Comparison of the root microbiota in two fields.

(**a**,**b**) Unconstrained (**a**) and constrained (**b**) principal coordinate analysis of *indica* in field I, *japonica* in field I, *indica* in field II, and *japonica* in field II with Bray-Curtis distance. (**c**,**d**) Principal coordinate analysis of *indica* in field I, *japonica* in field I, *indica* in field II, and *japonica* in field II with unweighted (**c**) and weighted UniFrac (**d**) distance. Ellipses cover 68% of the data for each rice subspecies. The numbers of replicated samples are as follows: in field I, *indica* (*n* = 201), *japonica* (*n* = 80); in field II, *indica* (*n* = 201), *japonica* (*n* = 81).

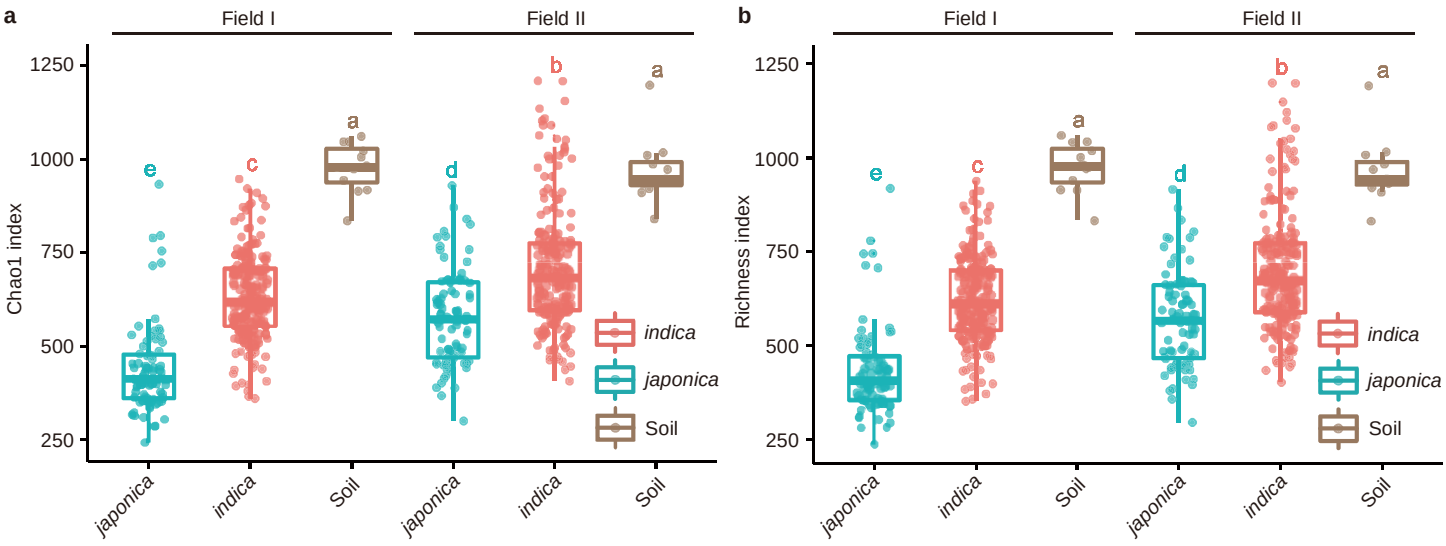

Supplementary Figure 4

Comparison of within-sample diversity (α-diversity) between *indica* and *japonica*.

(**a**,**b**) Chao 1 (**a**) and observed OTUs (**b**) of the root microbiota of *indica*, *japonica*, and corresponding unplanted bulk soils in two fields. The numbers of replicated samples are as follows: in field I, *indica* (*n* = 201), *japonica* (*n* = 80), soil (*n* = 12); in field II, *indica* (*n* = 201), *japonica* (*n* = 81), soil (*n* = 12). Data in two locations show the consistent trend that the root microbiota of *indica* show higher alpha diversity than those of *japonica*. The horizontal bars within boxes represent median. The tops and bottoms of boxes represent 75th and 25th percentiles, respectively. The upper and lower whiskers extend to data no more than 1.5 × the interquartile range from the upper edge and lower edge of the box, respectively.

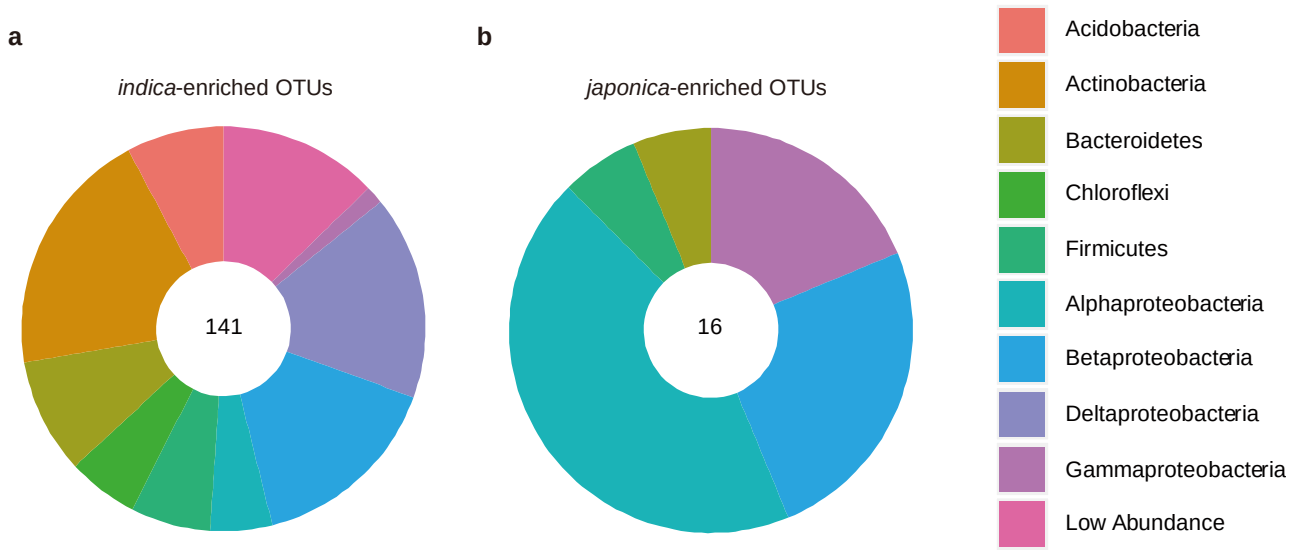

Supplementary Figure 5

Taxonomic composition of the *indica*- and *japonica*-enriched OTUs..

(**a**,**b**) The relative abundance of *indica*-enriched (**a**) and *japonica*-enriched (**b**) OTUs at the phylum level. Proteobacteria are shown at the class level.

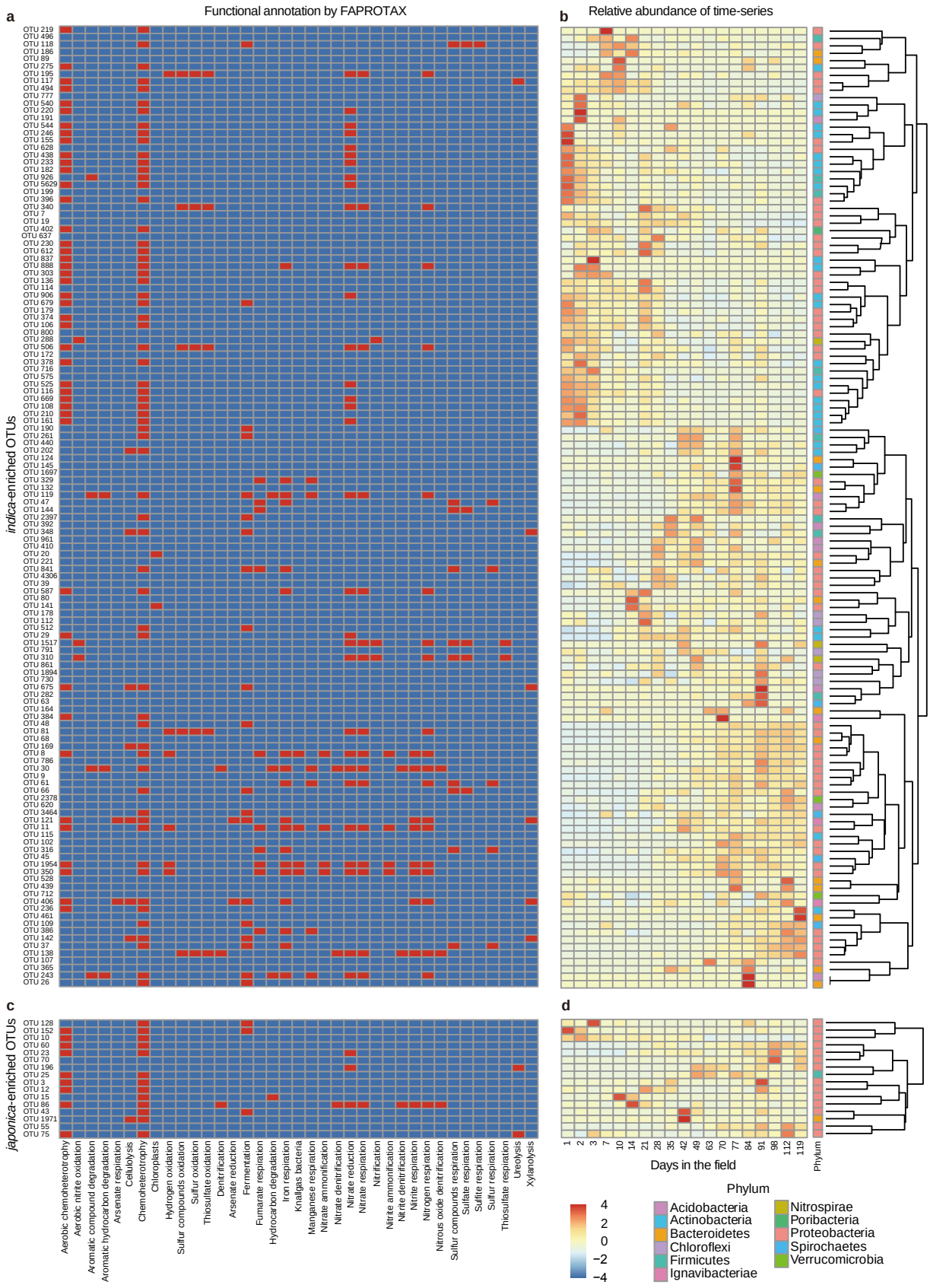
a
Functional annotation by FAPROTAX
indica-enriched OTUs
b
Relative abundance of time-series
c
japonica-enriched OTUs
d
Aerobic chemoheterotrophy
Aerobic nitrite oxidation
Aromatic compound degradation
Aromatic hydrocarbon degradation
Arsenate respiration
Cellulolysis
Chemoheterotrophy
Chloroplasts
Hydrogen oxidation
Sulfur compounds oxidation
Sulfur oxidation
Thiosulfate oxidation
Denitrification
Arsenate reduction
Fermentation
Fumarate respiration
Hydrocarbon degradation
Iron respiration
Knallgas bacteria
Manganese respiration
Nitrate ammonification
Nitrate denitrification
Nitrate reduction
Nitrate respiration
Nitrification
Nitrite ammonification
Nitrite denitrification
Nitrite respiration
Nitrogen respiration
Nitrous oxide denitrification
Sulfur compounds respiration
Sulfate respiration
Sulfite respiration
Sulfur respiration
Thiosulfate respiration
Ureolysis
Xylanolysis
Days in the field
Phylum
Acidobacteria
Actinobacteria
Bacteroidetes
Chloroflexi
Firmicutes
Ignavibacteriae
Nitrospirae
Poribacteria
Proteobacteria
Spirochaetes
Verrucomicrobia

Supplementary Figure 6

Function and time-series shift of the *indica*- and *japonica*-enriched OTUs.

(**a**) Functional annotation of *indica*-enriched OTUs by FAPROTAX. The presence of functions is shown in red. (**b**) Shift of relative abundance of *indica*-enriched OTUs according to time-course data from the rice root microbiota in the field in Changping Farm[17]. (**c**) Functional annotation of *japonica*-enriched OTUs by FAPROTAX. The presence of functions is shown in red. (**d**) Shift of relative abundance of *japonica*-enriched OTUs according to time-course data from the rice root microbiota in the field in Changping Farm[17].

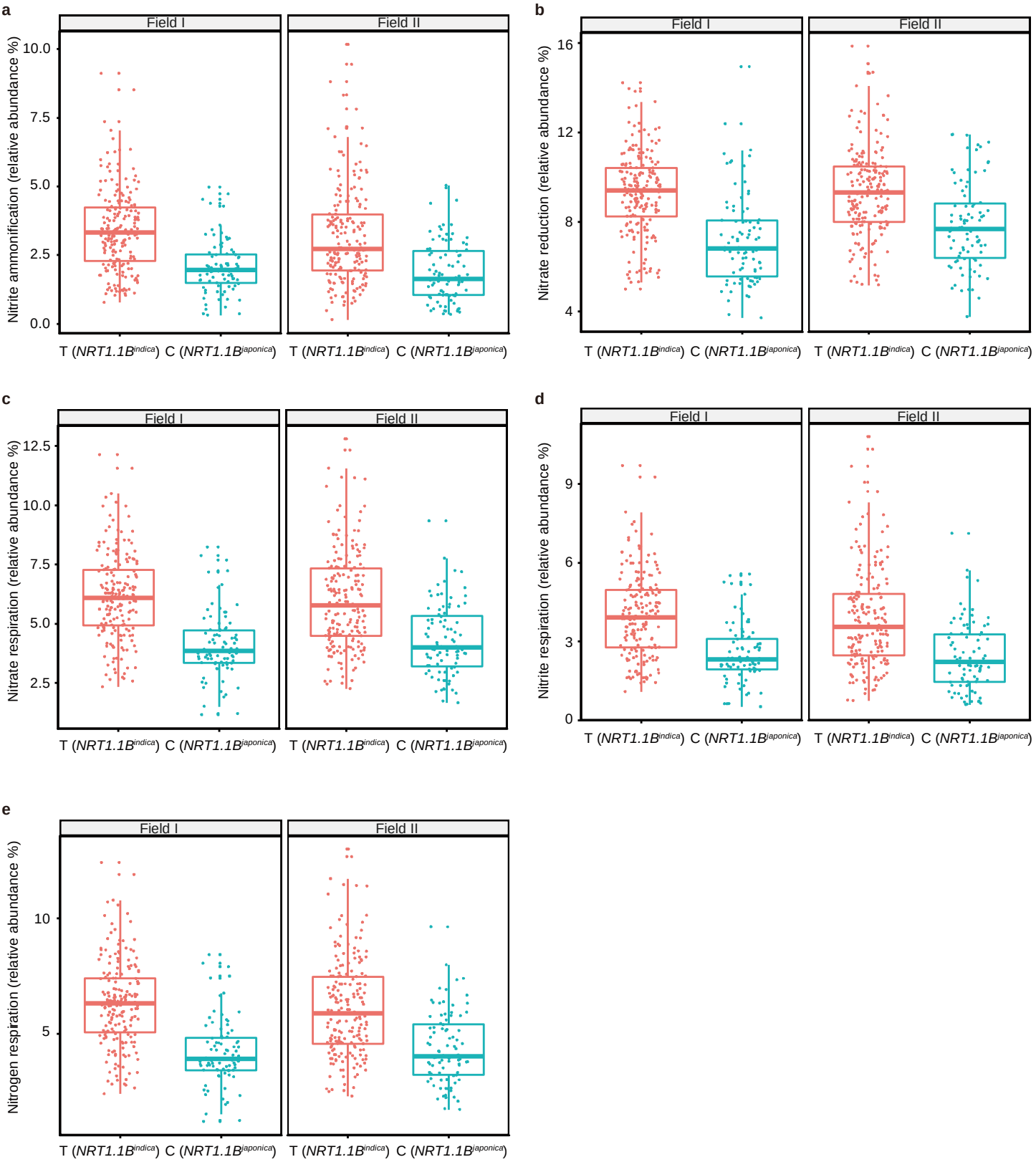

Supplementary Figure 7

Correlation between the natural variation of *NRT1.1B* and nitrogen-related functions in *indica* and *japonica* populations.

(**a**–**e**) The natural variation in *NRT1.1B* in *indica* and *japonica* populations is correlated with nitrogen-related functions in root microbiota from *indica* and *japonica* populations, including nitrite ammonification (**a**) ($P = 2.2 \times 10^{-16}$ in field I; $P = 1.8 \times 10^{-12}$ in field II, two-sided *t*-test), nitrate reduction (**b**) ($P = 1.1 \times 10^{-13}$ in field I; $P = 2.1 \times 10^{-8}$ in field II, two-sided *t*-test), respiration of nitrate (**c**) ($P = 2.2 \times 10^{-16}$ in field I; $P = 6.1 \times 10^{-13}$ in field II, two-sided *t*-test), nitrite respiration (**d**) ($P = 2.4 \times 10^{-16}$ in field I; $P = 7.2 \times 10^{-13}$ in field II, two-sided *t*-test) and nitrogen respiration (**e**) ($P = 2.2 \times 10^{-16}$ in field I; $P = 6.8 \times 10^{-13}$ in field II, two-sided *t*-test). $NRT1.1B^{indica}$ harbors a “T” at 980 bp downstream of the ATG start codon and $NRT1.1B^{japonica}$ harbors a “C” at the same position, resulting in an amino acid substitution (p. Met327Thr). The numbers of replicated samples are as follows: in field I, *indica* ($n = 192$), *japonica* ($n = 86$); in field II, *indica* ($n = 192$), *japonica* ($n = 87$).

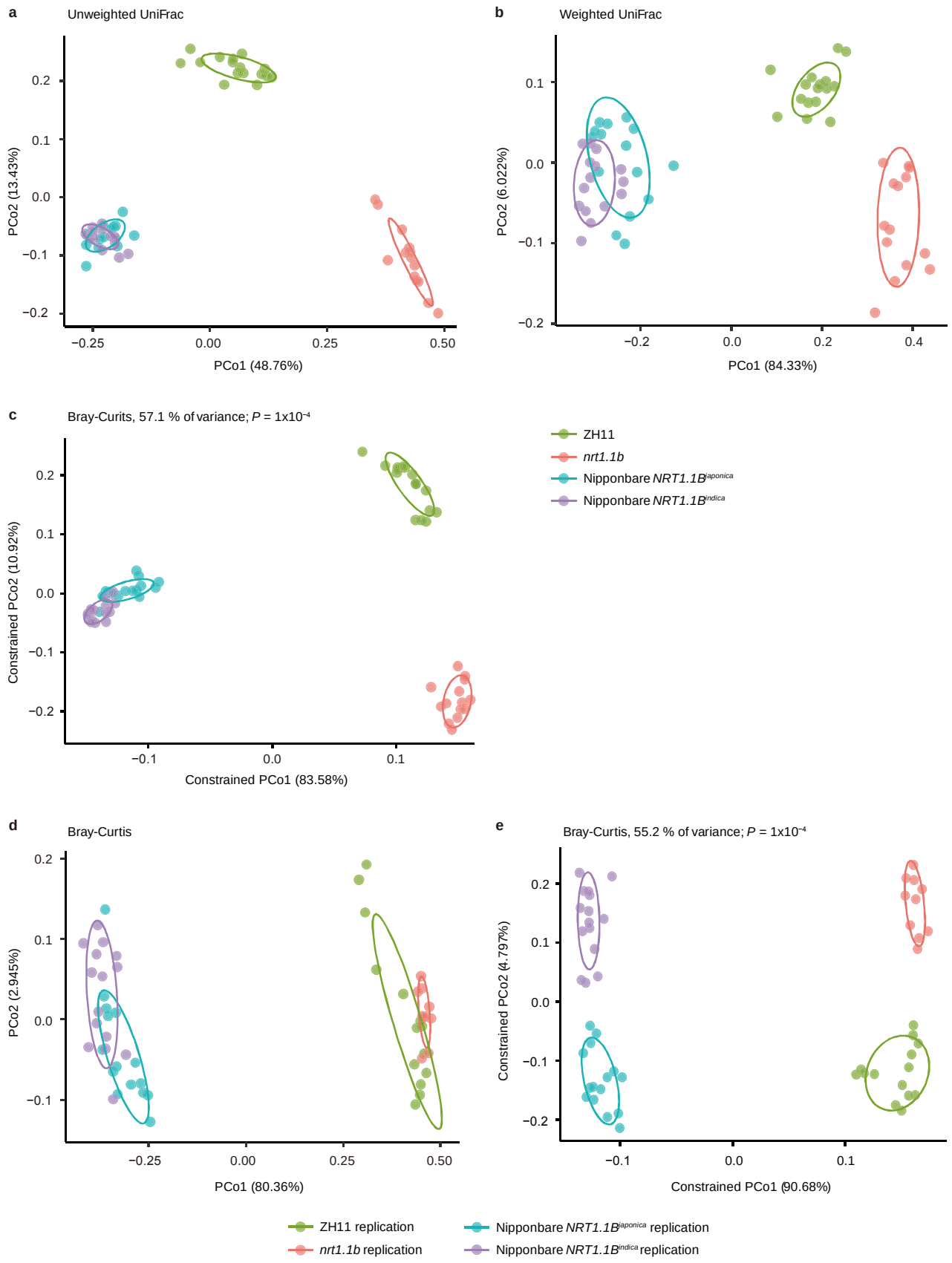
a
Unweighted UniFrac
PCo2 (13.43%)
PCo1 (48.76%)
b
Weighted UniFrac
PCo2 (6.022%)
PCo1 (84.33%)
c
Bray-Curits, 57.1 % of variance; P = 1x10⁻⁴
Constrained PCo2 (10.92%)
Constrained PCo1 (83.58%)
ZH11
nrt1.1b
Nipponbare NRT1.1B^japonica
Nipponbare NRT1.1B^indica
d
Bray-Curtis
PCo2 (2.945%)
PCo1 (80.36%)
e
Bray-Curtis, 55.2 % of variance; P = 1x10⁻⁴
Constrained PCo2 (4.797%)
Constrained PCo1 (90.68%)
ZH11 replication
nrt1.1b replication
Nipponbare NRT1.1B^japonica replication
Nipponbare NRT1.1B^indica replication

Supplementary Figure 8

NRT1.1B and its natural variation modulate the assembly of the rice root microbiota.

(**a**,**b**) Principal coordinate analysis with unweighted (**a**) and weighted (**b**) UniFrac distance showing that the root microbiota of ZH11 (wild-type), *nrt1.1b*, Nipponbare *NRT1.1B*^{indica}, and Nipponbare *NRT1.1B*^{japonica} separate in the first two axes. Ellipses cover 68% of the data for each genotype. (**c**) Constrained principal coordinate analysis showing that 57.1% of the root microbiota variations are explained by genotypes (ZH11, *nrt1.1b*, *NRT1.1B*^{indica}, and *NRT1.1B*^{japonica}). The numbers of replicated samples are as follows: ZH11 (n = 16), *nrt1.1b* (n = 14), *NRT1.1B*^{indica} (n = 15), *NRT1.1B*^{japonica} (n = 15). (**d**,**e**) A full factorial replication experiment validates the conclusion that *NRT1.1B* and its natural variation modulate the assembly of the rice root microbiota. Unconstrained (**d**) and constrained (**e**) principal coordinate analysis with Bray-Curtis distance showing that the root microbiota of ZH11 (wild-type), *nrt1.1b*, *NRT1.1B*^{indica}, and *NRT1.1B*^{japonica} separate in the first two axes. The plants were grown in different fields and at different time from the samples in **Fig. 4**. Ellipses cover 68% of the data for each genotype. The numbers of replicated samples are as follows: ZH11 (n = 14), *nrt1.1b* (n = 10), *NRT1.1B*^{indica} (n = 15), *NRT1.1B*^{japonica} (n = 15).

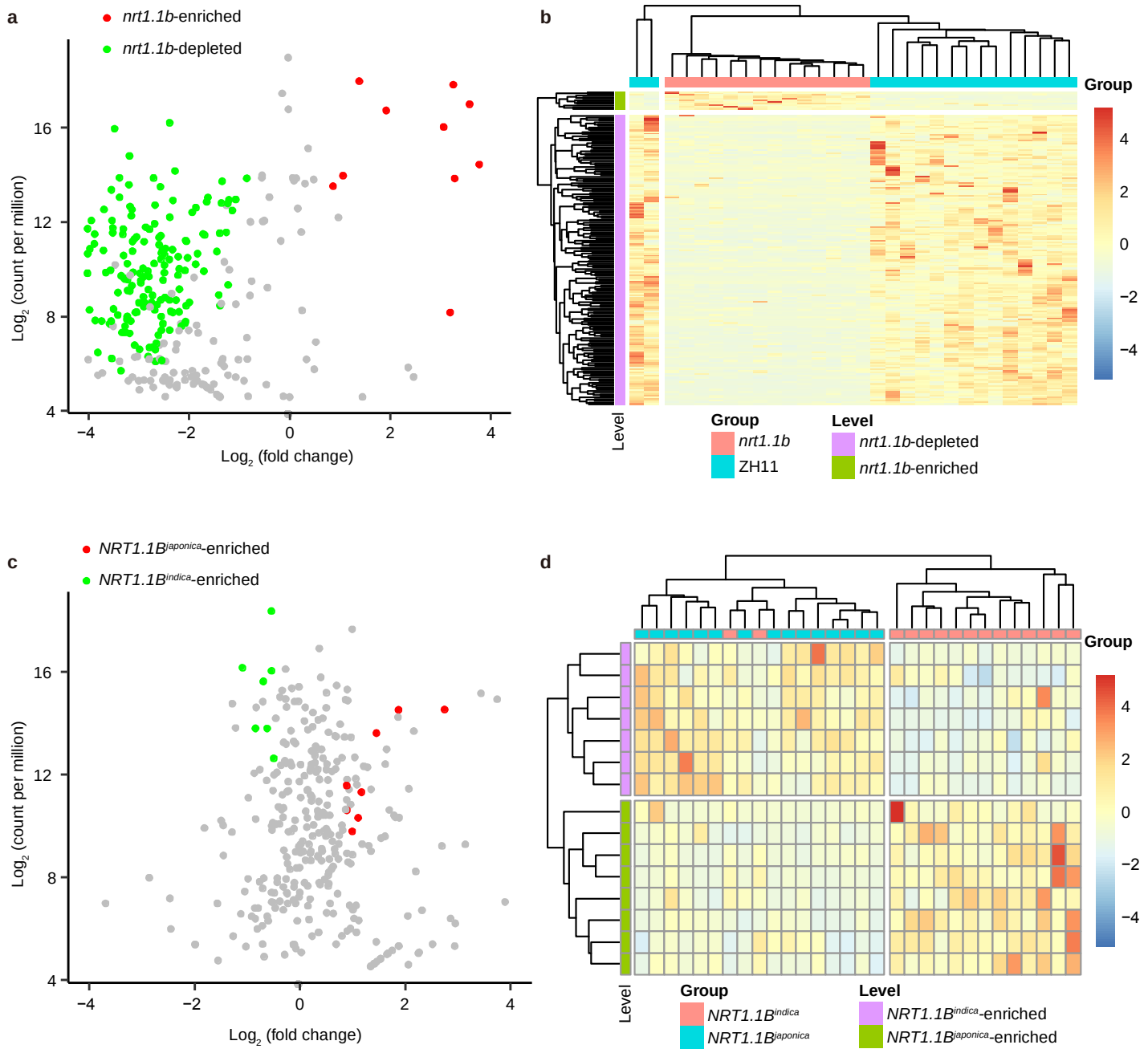

Supplementary Figure 9

OTUs associated with *NRT1.1B* in the field condition related to Fig. 4.

(**a**) Enrichment and depletion of OTUs in the *nrt1.1b* mutant compared with wild-type ZH11. Each point represents an individual OTU, and the position along the x axis represents the abundance fold change between the *nrt1.1b* mutant and wild-type. (**b**) Heat map showing the relative abundance of the differential OTUs between the *nrt1.1b* mutant and wild-type ZH11. (**c**) OTUs enriched in *NRT1.1B*^{indica} or *NRT1.1B*^{japonica}. Each point represents an individual OTU, and the position along the x axis represents the abundance fold change between *NRT1.1B*^{indica} or *NRT1.1B*^{japonica}. (**d**) Heat map showing the relative abundance of the differential OTUs between *NRT1.1B*^{indica} and *NRT1.1B*^{japonica}. The numbers of replicated samples are as follows: ZH11 (*n* = 16), *nrt1.1b* (*n* = 14), *NRT1.1B*^{indica} (n = 15), and *NRT1.1B*^{japonica} (n = 15).

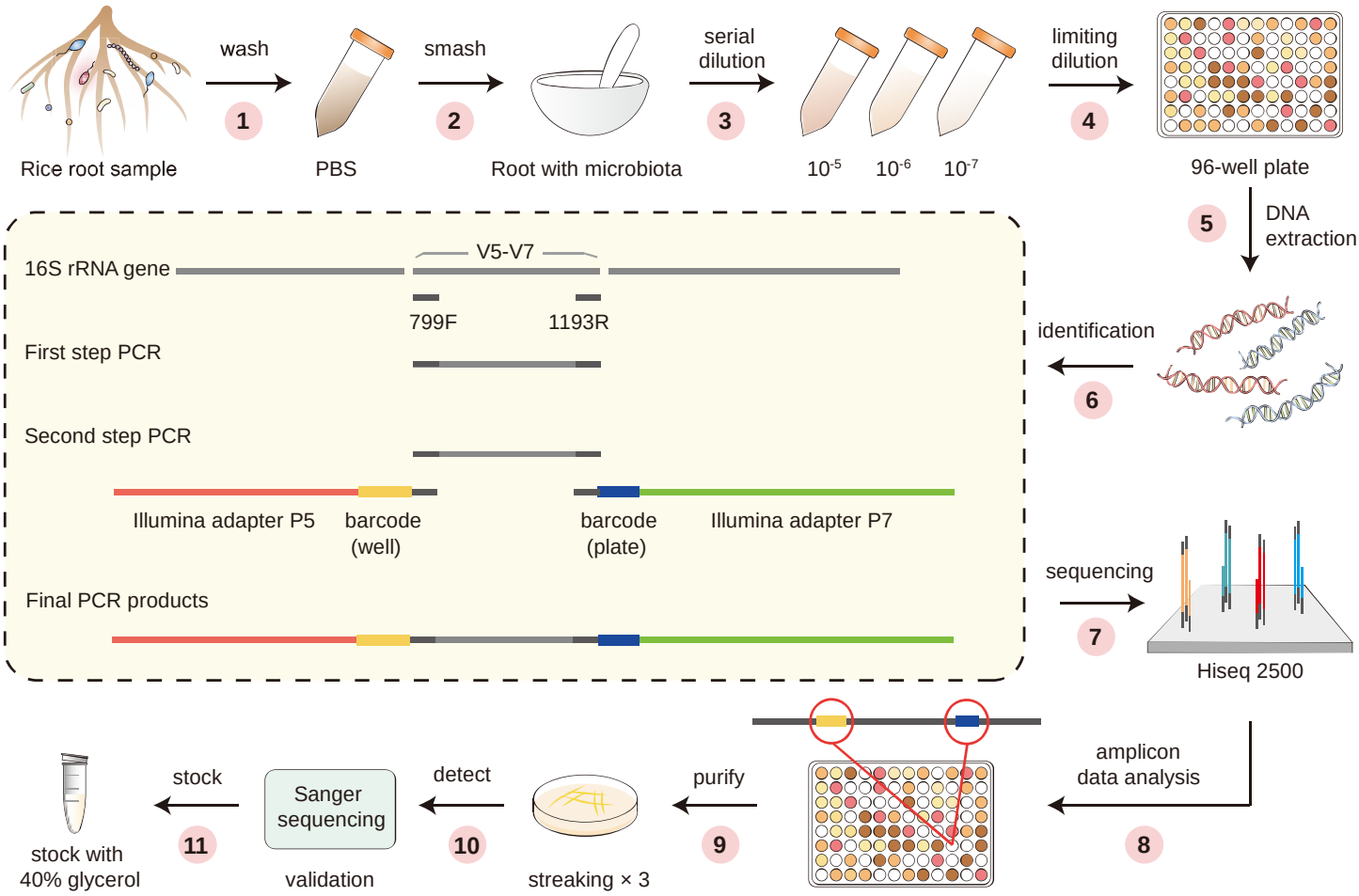

Supplementary Figure 10

Experimental procedure for isolation and identification of rice root-associated bacteria.

Step 1–4 illustrate the isolation procedure; Step 5–11 illustrate the identification of cultivated rice root-associated bacteria by the improved two-step barcoded system.

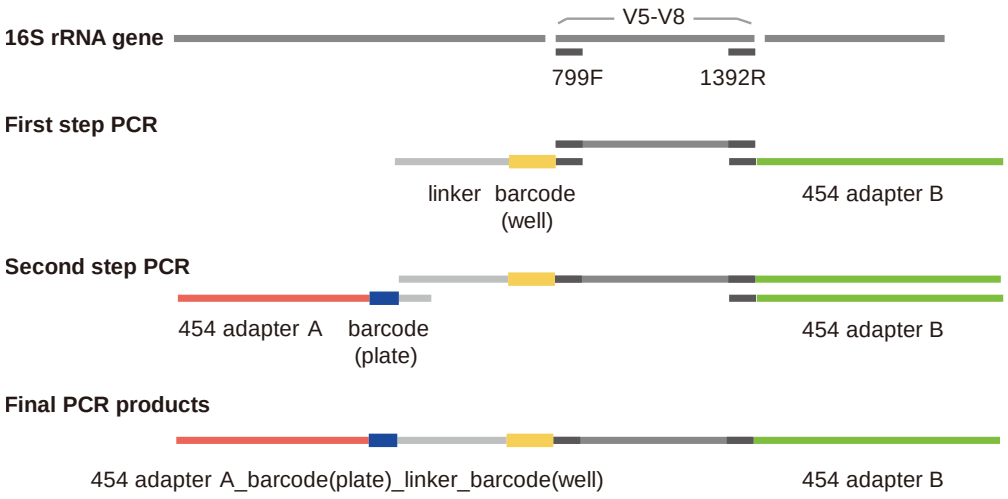

Supplementary Figure 11

The scheme for the previous high-throughput barcoding system to determine 16S rRNA gene sequences covering regions V5–V7 of bacterial isolates.

A previously published two-step barcoded pyrosequencing procedure (Bai, Y. *et al*. Functional overlap of the *Arabidopsis* leaf and root microbiota. *Nature* **528**, 364–369, 2015). Please note that the second step PCR generates chimera sequences that will contain mislabeled plate and well barcodes for bacterial identification.

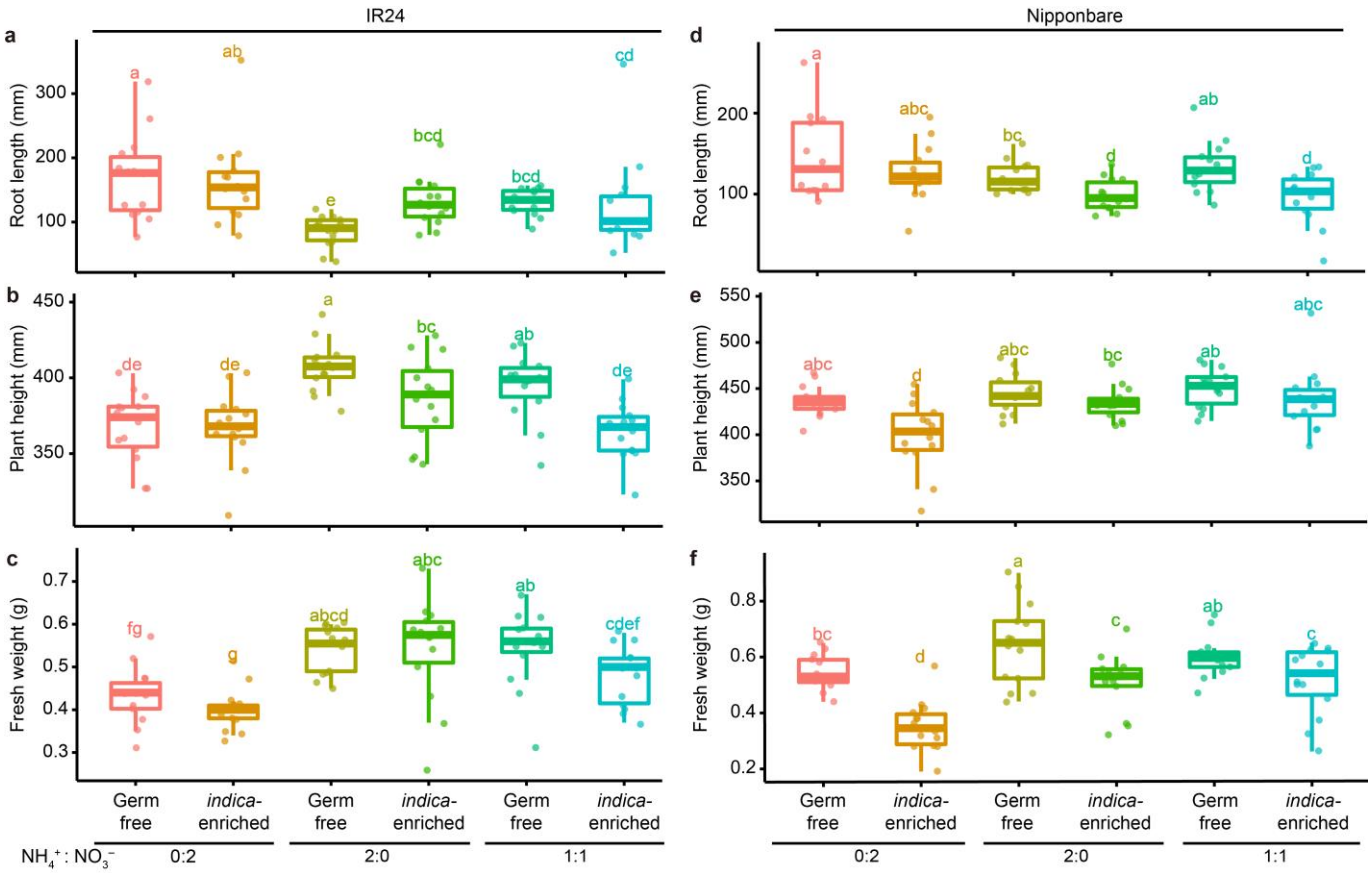

Supplementary Figure 12

Plant growth with or without *indica*-enriched SynCom under inorganic nitrogen conditions.

(**a**–**c**) IR24 (*indica*) rice plants were grown under different ratios of ammonium and nitrate (0:2, 2:0, and 1:1) with or without *indica*-enriched SynCom. After 2-week bacterial inoculation, rice plants were measured by root length (**a**), plant height (**b**), and shoot fresh weight (**c**). (**d**–**f**) Nipponbare (*japonica*) rice plants were grown under different ratios of ammonium and nitrate (0:2, 2:0, and 1:1) with or without *indica*-enriched SynCom. After 2-week bacterial inoculation, rice plants were measured by root length (**d**), plant height (**e**), and shoot fresh weight (**f**). Different letters indicate significantly different groups ($P < 0.05$, ANOVA, Tukey-HSD). Boxplots show combined data from three independent inoculation experiments with 4–5 technical replicates each (**Supplementary Table 13**). The horizontal bars within boxes represent medians. The tops and bottoms of boxes represent 75th and 25th percentiles, respectively. The upper and lower whiskers extend to data no more than 1.5 × the interquartile range from the upper edge and lower edge of the box, respectively.

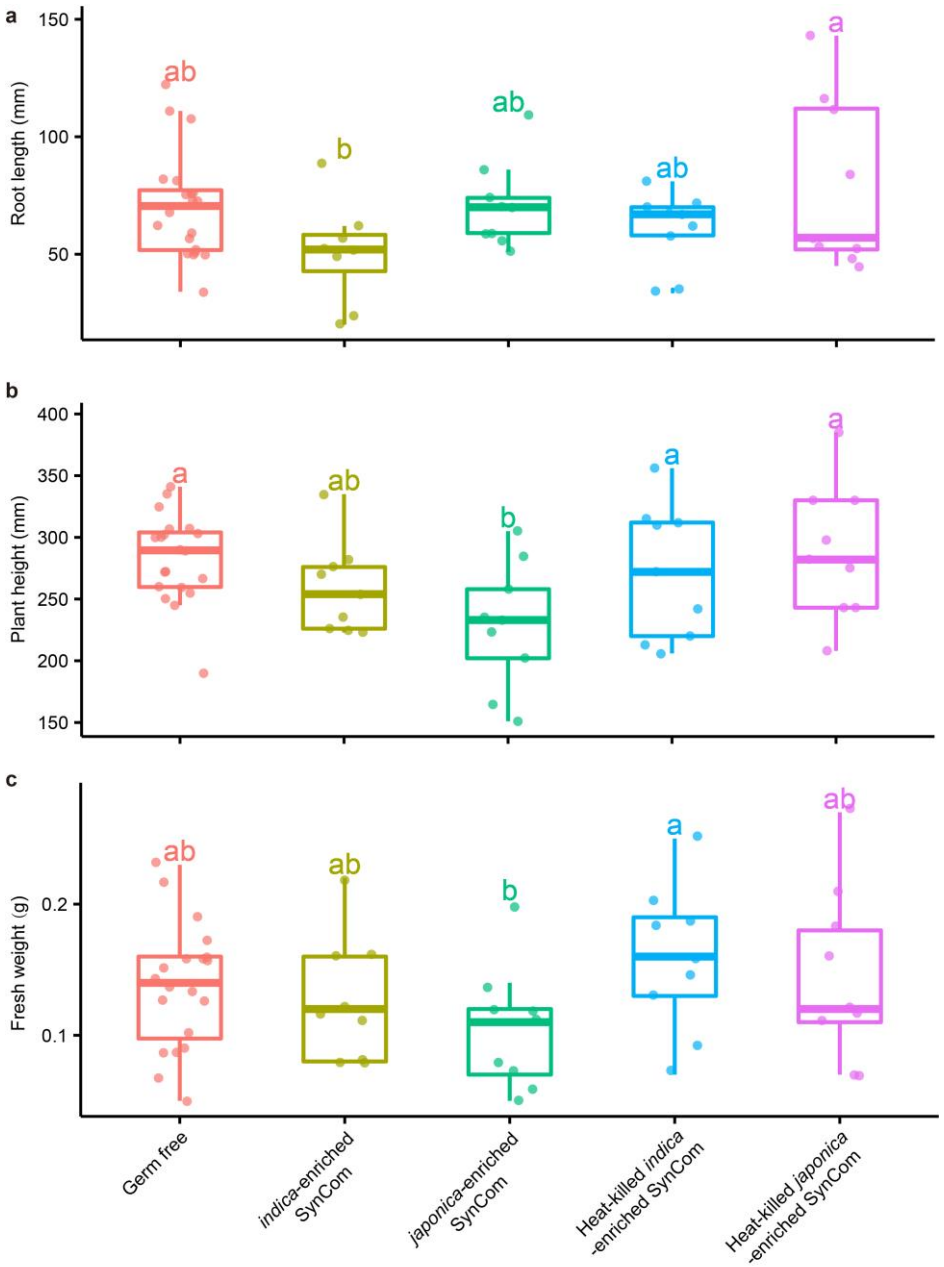

Supplementary Figure 13

Plant growth with *indica*- or *japonica*-enriched SynCom under inorganic nitrogen conditions.

IR24 rice plants were grown under the inorganic nitrogen condition with and without SynComs, including *indica*-enriched SynCom, *japonica*-enriched SynCom, and corresponding heat-killed bacteria as controls, respectively (**Supplementary Table 13**). After 2-week bacterial inoculation, rice plants were measured by root length (**a**), plant height (**b**), and shoot fresh weight (**c**). Different letters indicate significantly different groups ($P < 0.05$, ANOVA, Tukey-HSD). Boxplots show combined data from two independent inoculation experiments with 4–5 technical replicates each. The horizontal bars within boxes represent medians. The tops and bottoms of boxes represent 75th and 25th percentiles, respectively. The upper and lower whiskers extend to data no more than 1.5 × the interquartile range from the upper edge and lower edge of the box, respectively.